Synthetic Metals 161 (2011) 1699–1706

Contents lists available at ScienceDirect

Synthetic Metals

journal homepage: www.elsevier.com/locate/synmet

Design and synthesis of a new thiophene based donor–acceptor type conjugated polymer with large third order nonlinear optical activity

K.A. Vishnumurthy[a], A. Vasudeva Adhikari[a,*], M.S. Sunitha[a], K.A. Ann Mary[b], Reji Philip[b]

[a] Department of Chemistry, National Institute of Technology Karnataka, Surathkal, Mangalore 575 025, India
[b] Light and Matter Physics Group, Raman Research Institute, C.V. Raman Avenue, Sadashiva Nagar, Bangalore 560 080, India

ARTICLE INFO

Article history:
Received 21 December 2010
Received in revised form 7 April 2011
Accepted 4 June 2011
Available online 7 July 2011

Keywords:
Donor–acceptor polymer
3,4-Dialkoxythiophene
Thienylene-vinylene
Oxadiazole
NLO properties
DFWM

ABSTRACT

In this communication we describe the design and synthesis of a new conjugated polymer (**P**) carrying 3,4-dialkoxythiophene, 1,3,4-oxadiazole and thienylene-vinylene units, from its monomers using Wittig condensation method. The structure of newly synthesized polymer was confirmed by FT-IR, ^{1}H NMR, UV–vis spectral, elemental analysis and gel permeation chromatographic techniques. The polymer exhibited good thermal stability with the onset decomposition temperature around 320 °C in nitrogen atmosphere. Further, its electrochemical, linear and nonlinear optical properties have been investigated. The optical and electrochemical band gap was found to be 2.21 eV. Its third-order nonlinear optical property was investigated by *Z*-scan and DFWM techniques, using a Q-switched, frequency doubled Nd:YAG laser producing 7 ns laser pulses at 532 nm. *Z*-scan results reveal that the polymer exhibits self-defocusing nonlinearity. The operating mechanism involves reverse saturable absorption. The polymer shows strong optical limiting behavior due to effective two-photon absorption (2PA). The value of 2PA coefficient was found to be 3.0×10^{-11} mW, which is comparable to that of good optical limiting materials. The fluorescence quantum yield of the polymer in solution was determined using quinine sulfate as standard and it was found to be 35%.

1. Introduction

Polymeric nonlinear optical (NLO) materials have been identified as strong candidates for use in a variety of photonic devices, including high-speed optical modulators, ultrafast optical switches and high-density optical data storage media [1–3], which are essential for continued advancement in the effort to transform information storage and transmission from the electrical to the optical regime. The promise of NLO active polymers lies in their fortuitous combination of exceptional optical quality, low cost and ease of fabrication into device structures. This juxtaposition of technologically favorable aspect has led to considerable research activities towards the development of new NLO active polymers for commercial applications. One of the major challenges in this research area is to design and synthesize the NLO active chromophores exhibiting large molecular hyperpolarizability (β) and high thermal stability. It has been well established that many conjugated polymeric systems carrying aromatic heterocyclic rings exhibit an increased hyperpolarizability when compared to those carrying benzenoid systems [2,4,5]. This is because of the fact that delocalization energy of heteroaromatics is lower than that of benzenoid systems. Chromophores containing aromatic heterocycles such as thiophene [6–8], thiazole [9,10], benzothiazole [10,11] and benzoxazole [12,13] or their derivatives are among the most studied systems.

Recently Cassano et al. [14] reported a new strategy for tuning nonlinear optical properties of the π-conjugated polymers. According to them, incorporation of alternate electron-acceptor and electron-donor units along the polymer main chain would enhance the NLO properties significantly, mainly due to hyperpolarizability. The desired optical properties can be achieved when new conjugated systems are composed of donor–acceptor (D–A) segments with different heterocyclic systems which allow the fine tuning of important physical and/or photophysical properties. Such aromatic D–A type molecules with push–pull mechanism are quite stable and they exhibit reasonably good β values. It has been reported that incorporation of benzene rings into the aliphatic push–pull polyenes leads to saturate molecular nonlinearity [15]. Further, oligothiophenes have been shown to possess better electron relay properties and hence larger contributions to β values than that of polyenes. Also, oligothiophenes have a strong tendency to increase β values with increasing number of thiophene units. Besides the electron transmission efficiency, oligothiophenes possess inherent stability [16]. An extensive literature survey reveals that 3,4-dialkoxy thiophene based conjugated

* Corresponding author. Tel.: +91 8242474046; fax: +91 8242474033.
E-mail addresses: avadhikari123@yahoo.co.in, avchem@nitk.ac.in (A.V. Adhikari).

0379-6779/$ – see front matter © 2011 Elsevier B.V. All rights reserved.
doi:10.1016/j.synthmet.2011.06.007

polymers show facile dopability and low band gap ascribe to the electron donating nature of the alkoxy moiety. It has been also reported that introduction of long alkoxy pendants at 3- and 4-positions of the thiophene ring improves the solvent processibility and hole carrying ability of the corresponding polymer. Further, the incorporation of highly electron withdrawing oxadiazole ring along the conjugation path increases the charge carrying property of the polymer [17,18]. In addition to this, introduction of vinylene linkages increases the planarity of the polymer chain by reducing the torsional interactions between the hetero aromatic rings, which leads to decrease in the band gap [19].

Against this background, we have designed a new D–A type conjugated polymer **P**, viz. Poly 2-(5-(1,3,4-oxadiazol-2-yl)-3,4-bis(tetradecyloxy)thiophen-2-yl)-5-((E)-2-(5-(4-(5-(3,4-bis (dodecyloxy)-5-(1,3,4-oxadiazol-2-yl)thiophen-2-yl)-1,3,4-oxadiazol-2-yl)styryl)thiophen-2-yl)vinyl)-1,3,4-oxadiazole, wherein additional unsubstituted thiophene moiety with vinylic linkage has been introduced in between electron donating 3,4-dialkoxy substituted thiophene and electron accepting 1,3,4-oxadiazole systems, in order to reduce the steric repulsion between the bulky alkoxy groups and to increase planarity of the polymer chain that could help to reduce the band gap. It has been predicted that introduction of thienylene-vinylene group would increase the conjugation path length and hence bring about enhanced optical limiting behavior of the resulting polymer. Accordingly, the new polymer has been synthesized in good yield from its monomers following Wittig condensation method. The required monomers have been prepared from simple thiodiglycolic acid through multistep reactions. The structure of the new polymer has been established by spectral techniques and further its electrochemical, optical and nonlinear optical properties have been evaluated in order to investigate the influence of its structure on the properties.

2. Experimental

2.1. Materials and methods

3,4-Dialkoxythiophene-2,5-dicarbohydrazide (**6a,b**) were synthesized according to the reported procedure [17]. Dimethylformamide and acetonitrile were dried over CaH_2. Thiodiglycolic acid, diethyl oxalate, tetrabutyl ammonium perchlorate (TBAPC) and *n*-bromododecane and *n*-bromotetradecane were purchased from Lanchaster (UK) and were used as received. All the solvents and reagents were of analytical grade. They were purchased commercially and used without further purification.

2.2. Instrumentation

Infrared spectra of all intermediate compounds and polymer were recorded on a Nicolet Avatar 5700 FTIR (Thermo Electron Corporation). The UV–visible and fluorescence spectra were taken in GBC Cintra 101 UV–visible and Perkin Elmer LS55 fluorescence spectrophotometers, respectively. ^{1}H NMR spectra were obtained with Bruker-400 MHz FT-NMR spectrometer using TMS/solvent signal as internal reference. Elemental analyses were performed on a Flash EA1112 CHNS analyzer (Thermo Electron Corporation). Mass spectra were recorded on a Jeol SX-102 (FAB) Mass Spectrometer. The electrochemical studies of the polymer were carried out using AUTOLAB PGSTAT30 electrochemical analyzer. Cyclic voltammagram was recorded using a three-electrode cell system, with glassy carbon button as working electrode, a platinum wire as counter electrode and an Ag/AgCl electrode as the reference electrode. Molecular weights of the polymer were determined with a WATERs make gel permeation chromatograph (GPC) against polystyrene standards with tetrahydrofuran (THF) as an eluent. The third-order NLO properties of these polymer were studied at 532 nm in THF solution with 7 ns pulses from an Nd:YAG laser using the *Z*-scan and degenerate four wave mixing (DFWM) techniques.

2.2.1. Z-scan measurement

The *Z*-scan technique [20] was developed to simultaneously measure the magnitude of both the nonlinear refraction (NLR) and the nonlinear absorption (NLA). The sign of the nonlinear refractive index (n_2) can also be obtained at the same time. In the "open aperture" *Z*-scan, which provides information about the nonlinear absorption coefficient, a laser beam is used for molecular excitation and its propagation direction is taken as the *z*-axis. The beam is focused using a convex lens and the focal point is taken as $z = 0$. The beam has maximum energy density at the focus, and the energy density drops symmetrically on either side of the focus (i.e., for positive and negative values of z). In the experiment, the sample is placed in the beam at different positions with respect to the focus (different values of z), and the corresponding transmission is measured. The sample sees different laser intensity at each position, and therefore its position-dependent transmission will give information on its intensity-dependent transmission as well. The nonlinear absorption coefficient can be calculated from this nonlinear transmission information.

We used a stepper-motor-controlled linear translation stage in our setup to move the sample through the beam in precise steps. The sample was placed in a 1 mm cuvette. The transmission of the sample at each point was measured using two pyroelectric energy probes (Rj7620, Laser Probe Inc., Utica, NY, USA). One energy probe monitored the input energy while the other monitored the energy transmitted through the sample. The second harmonic output (532 nm) of a Q-switched Nd:YAG laser (Quanta Ray, Spectra Physics) was used to excite the molecules. The temporal width (FWHM) of the laser pulses was 7 ns. Laser pulse energy of 160 μJ was used for the experiments. The pulses were fired in the "single shot" mode, allowing sufficient time between successive pulses to avoid accumulative thermal effects in the sample.

2.2.2. DFWM studies

Degenerate four-wave mixing (DFWM) is a commonly used technique to determine the magnitude and temporal dynamics of the third-order nonlinearity of a medium [21–24]. This process involves the nonlinear mixing of three spatially distinguishable beams to produce a fourth beam that has a different propagation direction than the original beams. When all the waves have the same frequency, it is called degenerate four-wave mixing (DFWM). Usually two configurations, namely the phase-conjugate and BOXCARS geometries, are used for DFWM experiments. We used the forward folded BOXCARS geometry, where a laser beam is split into three and the beams are aligned such that they form three corners of a square. The diametrically opposite beams are the pump beams, and they have the same intensity. The third beam is the probe, which has an intensity of about 20% of the pump beam. When the beams are focused onto the sample the fourth beam (signal beam) is generated due to nonlinear interaction, which will appear on the fourth corner of the square. It can be measured using a detector. In our DFWM experiment we used 7 ns pulses at 532 nm obtained from the second harmonic output of a Q-switched Nd:YAG laser. A rotating polarizer was used to change the intensity of the input laser beam. The sample was taken in a 2 mm glass cuvette. The input energy was monitored using a pyroelectric energy probe. The generated signal beam was measured in the far field using a calibrated photodiode.

2.3. Synthesis of intermediates, monomers and polymer

2.3.1. Synthesis of 3,4-dialkoxythiophene-2,5-carboxydihydrazides [6a,b]

Diethyl 3,4-dialkoxythiophene-2,5-dicarboxylate (0.5 g) was added to a solution of 5 mL hydrazine monohydrate in 40 mL of ethanol. The reaction mixture was refluxed for 3 h. Upon cooling the solution to room temperature a white precipitate was obtained. The precipitate was filtered, washed with petroleum ether, dried under vacuum and finally recrystallized from ethanol to get crystalline white crystalline solid. **6a**: Yield: 92%. IR (KBr, cm^{-1}): 3412 ($-NH_2$), 3341 (–NH–), 2915, 2848, 1650 (–C=O), 1501, 1302, 1043, 956,720. **6b**: Yield: 86%. IR (KBr, cm^{-1}): 3411 ($-NH_2$), 3341 (–NH–), 2916, 2848, 1651 (–C=O), 1501, 1312, 1042, 956,721.

2.3.2. Synthesis of 3,4-bis(tetradecyloxy)-N′2,N′5-bis(3-(thiophen-2-yl)acryloyl)thiophene-2,5-dicarbohydrazide [7a]

To a mixture of compound **6a** (5 g, 8 mmol) and 2 mL of pyridine in 50 mL of NMP, 3-(thiophen-2-yl)acryloyl chloride (2.76 g, 16 mmol) was added slowly at room temperature while stirring. The stirring was continued at room temperature for 8 h. The reaction mixture was poured into excess of water to get a precipitate. The precipitate obtained was collected by filtration, washed with excess of water, dried in oven and recrystallized from ethanol/chloroform mixture. **7a**: Yield: 82%, m.p.: 210–212 °C. ^{1}H NMR (400 MHz, $CDCl_3$) δ (ppm): 7.74 (d, 2H, –CH=CH–, J = 16 Hz), 7.42 (d, 2H, Ar–H, J = 4.8 Hz), 7.29 (d 2H, Ar–H, J = 3.6), 7.10 (m, 2H, Ar–H), 6.9 (d, 2H, –CH=CH–, J = 16 Hz), 4.31 (t, 4H, –O–CH_2–, J = 7 Hz), 1.24–1.83 (m, 48H, –$(CH_2)_{10}$–), 0.89 (t, 6H, ACH_3, J = 6.8 Hz). IR (KBr, cm^{-1}): 3310, 3214, 2918, 2852, 1685, 1648, 1495, 1303, 1051, 931, 723. Element. Anal. Calcd. for $C_{48}H_{72}N_4O_6S_3$: C, 64.25; H, 8.09; N, 6.24; S, 10.72. Found: C, 64.34; H, 8.23; N, 6.29; S, 10.86.

2.3.3. Synthesis of 5,5′-(3,4-bis(tetradecyloxy)thiophene-2,5-diyl)bis(2-(-2-(thiophen-2-yl)vinyl)-1,3,4-oxadiazole) [8a]

A mixture of compound **7a** (3 g, 3.4 mmol) and 50 mL of phosphorous oxychloride was heated at 80 °C for 6 h. The reaction mixture was then cooled to room temperature and poured into crushed ice. The resulting precipitate was collected by filtration, washed with water and dried in oven. Further purification was done by column chromatography using silica gel using PE/EA as eluent. **8a**: Yield: 56%, m.p.: 189–190 °C. ^{1}H NMR (400 MHz, $CDCl_3$) δ (ppm): 7.74 (d, 2H, –CH=CH–, J = 16 Hz), 7.42 (d, 2H, Ar–H, J = 4.8 Hz), 7.29 (d 2H, Ar–H, J = 3.6), 7.10 (m, 2H, Ar–H), 6.9 (d, 2H, –CH=CH–, J = 16 Hz), 4.31 (t, 4H, –O–CH_2–, J = 7 Hz), 1.24–1.83 (m, 48H, –$(CH_2)_{10}$–), 0.89 (t, 6H, Ar–CH_3, J = 6.8 Hz). IR (KBr, cm^{-1}): 2916, 2849, 1585 (–C=N–), 1458, 1274, 1044, 955, 712. Element. Anal. Calcd. for $C_{48}H_{68}N_4O_4S_3$: C, 66.94; H, 7.96; N, 6.51; S, 11.17. Found: C, 67.04; H, 7.99; N, 6.65; S, 11.24.

2.3.4. Synthesis of 2,2′-(5,5′-(3,4-bis(tetradecyloxy)thiophene-2,5-diyl)bis(1,3,4-oxadiazole-5,2-diyl))bis(ethene-2,1-diyl)dithiophene-2-carbaldehyde [9a]

Dialdehyde **9a** was synthesized using the Vilsmeier–Haack reaction. *N*,*N*-Dimethylformamide (0.954 g, 13 mol) cooled to 0 °C was treated drop wise with phosphorus oxychloride (1.989 g, 13 mol). The resulting orange solution was stirred at 0 °C for 1 h and at 25 °C for 1 h, and then compound **8a** (2 g, 2.18 mmol) in 20 mL of 1,2-dichloroethane was added slowly. The mixture was heated at 90 °C for 24 h, cooled, and poured onto 200 g of crushed ice. Brown oil separated, which was taken up in dichloromethane. The extract was washed with saturated aqueous bicarbonate and then with water containing a little ammonium chloride and the organic layer was dried over anhydrous Na_2SO_4. The solvent was removed under reduced pressure, and the crude viscous product was separated on a silica gel column, using hexane:ethyl acetate (1:1) as eluent. The yield of the dialdehyde was 37%. ^{1}H NMR (400 MHz, $CDCl_3$) δ (ppm): 9.94 (s, 2H, Ar–CHO), 7.74 (m, 4H, –CH=CH–), 7.37 (d, 2H, Ar–H, J = 4.8 Hz), 7.11 (m, 2H, Ar–H), 4.31 (t, 4H, –O–CH_2–, J = 7 Hz), 1.85–1.24 (m, 48H, –$(CH_2)_{10}$–), 0.87 (t, 6H, Ar–CH_3, J = 6.8 Hz). IR (KBr, cm^{-1}): 2918, 2849, 1662 (–HC=O), 1590, 1458, 1354, 10044, 809, 720. Element. Anal. Calcd. for $C_{50}H_{68}N_4O_6S_3$: C, 65.47; H, 7.47; N, 6.11; S, 10.49. Found: C 65.55; H, 7.58; N, 6.23; S, 10.51.

2.3.5. Synthesis of N2,N5-di-(4-methylbenzoyl)-3,4-didodecyloxy thiophene-2,5-dicarbo hydrazide [10b]

To a clear mixture of dihydrazide **6b** (5 g, 8.79 mmol) and 2 mL of pyridine in 50 mL of NMP, 2 equiv. (2.71 g, 17.58 mmol) of 4-methyl benzoyl chloride was added slowly at room temperature while stirring. The stirring was continued at room temperature for 1 h. The resulting solution was heated at 80 °C for 5 h. After cooling to room temperature, the reaction mixture was poured into excess of water to get a precipitate. The precipitate obtained was collected by filtration, washed with excess of water, dried in oven and recrystallized from ethanol/chloroform mixture to get desired product. **10b**: Yield: 82%. FAB: m/z, 806, ^{1}H NMR (400 MHz, $CDCl_3$), δ (ppm): 10.22 (s, 2H, –NH–), 9.71 (s, 2H, –NH–), 7.75 (d, 4H, Ar, J = 8.4 Hz), 7.15 (d, 4H, Ar, J = 8.0 Hz), 4.24 (t, 4H, –OCH_2–, J = 7.0 Hz), 2.38 (s, 6H, Ar–CH_3), 1.12–1.84 (m, 40H, –$(CH_2)_{10}$–) 0.80 (t, 6H, ACH_3, J = 7.4 Hz). IR (KBr, cm^{-1}): 3245 (–CO–NH–), 2917, 2849 (Aromatic), 1666, 1621, 1447, 1274, 1046, 835, 732. Element. Anal. Calcd. for $C_{46}H_{68}N_4O_6S$: C, 68.62; H, 8.51; N, 6.96; S, 3.98. Found: C, 68.72; H, 8.64; N, 6.98; S, 4.01.

2.3.6. Synthesis of 2,2′-(3,4-dialkoxythiophene-2,5-diyl)bis[5-(4-methylphenyl)-1,3,4-oxadiazole] [11b]

A mixture of compound **10b** (5 g, 6.2 mmol) and 50 mL of phosphorous oxychloride was heated at 80 °C for 6 h. The reaction mixture was then cooled to room temperature and poured into an excess of ice cold water. The resulting precipitate was collected by filtration, washed with water and dried in oven. Further purification was done by recrystallization of the obtained solid from ethanol/chloroform mixture. **11b**: Yield: 85%, m.p.: 98–100 °C. ^{1}H NMR (400 MHz, $CDCl_3$) δ (ppm): 7.95 (d, 4H, Ar, J = 8.4 Hz), 7.28 (d, 4H, Ar, J = 8.0 Hz), 4.25 (t, 4H, –O–CH_2–, J = 6.6 Hz), 2.38 (s, 6H, Ar–CH_3), 1.13–1.83 (m, 40H, –$(CH_2)_{10}$–), 0.80 (t, 6H, Ar–CH_3, J = 7.0 Hz). IR (KBr, cm^{-1}): 2915, 2849, 1587 (–C=N–), 1557, 1482, 1465′, 1279, 1054, 822, 726. Element. Anal. Calcd. for $C_{46}H_{64}N_4O_4S$: C, 71.84; H, 8.39; N, 7.28; S, 4.17. Found: C, 71.72; H, 8.42; N, 7.31; S, 4.2.

2.3.7. Synthesis of 2,20-(3,4-dialkoxythiophene-2,5-diyl)bis[5-(4-bromomethylphenyl)-1,3,4-oxadiazole] [12b]

A mixture of compound **11b** (3 g, 3.9 mmol), *N*-bromosuccinimide (1.38 g, 7.8 mmol) and 5 mg of benzoyl peroxide in 30 mL of benzene was refluxed for 5 h. After the solvent was removed, 20 mL of water was added with stirring for 1 h. The resulting crude product was recrystallized from methyl acetate/chloroform mixture. 2,2′-(3,4-Ditetradecyloxythiophene-2,5-diyl)bis[5-(4-bromomethylphenyl)-1,3,4-oxadiazole]. **12b**: Yield: 65%. ^{1}H NMR (400 MHz, $CDCl_3$) δ (ppm): 7.92 (d, 4H, Ar, J = 8.4 Hz), 7.27 (d, 4H, Ar, J = 8.0 Hz), 4.5 (s, 4H, Ar–CH_2–Br), 4.24 (t, 4H, –O–CH_2–, J = 6.6 Hz), 1.13–1.83 (m, 40H, –$(CH_2)_{10}$–), 0.80 (t, 6H, Ar–CH_3, J = 7.0 Hz). IR (KBr, cm^{-1}): 2915, 2849, 1557 (–C=N–), 1482, 1465, 1279, 1054, 952, 822, 726. Element. Anal. Calcd. for

$C_{46}H_{62}Br_2N_4O_4S$: C, 59.61; H, 6.74; N, 6.04; S, 3.46. Found C, 59.68; H, 6.75; N, 6.1; S, 3.52.

2.3.8. Synthesis of 2,20-(3,4-ditetradecyloxythiophene-2,5-diyl)bis[5-((4-triphenylphosphonionmethyl)phenyl)-1,3,4-oxadiazole]dibromide [13b]

A solution of dibromide compound **12b** (1 g, 1.07 mmol) and triphenyl phosphine (0.565 g, 2.157 mmol) in 5 mL of DMF was refluxed with stirring for 10 h. The reaction mixture was cooled to room temperature and poured into 50 mL of ethyl acetate. The resulting precipitate was filtered off, washed with excess of ethyl acetate and dried at 40 °C for 10 h. **13b**: Yield: 72%, m.p.: above 300 °C. ^{1}H NMR (400 MHz, $CDCl_3$), δ (ppm): 7.20–7.90 (m, 38H, Ar–H), 5.95 (s, 4H, Ar–CH_2–P–), 4.25 (t, 4H, –OCH_2–, J = 6.9 Hz), 1.13–1.83 (m, 40H, –$(CH_2)_{10}$–), 0.79 (t, 6H, ACH_3, J = 7.0 Hz). IR (KBr, cm^{-1}): 2922, 2854, 1583, 1460, 1350, 1046, 956, 725. Element. Anal. Calcd. for $C_{82}H_{92}Br_2N_4O_4P_2S$: C, 67.85; H, 6.39; N, 3.86; S, 2.21. Found C, 67.92; H, 6.46; N, 3.92; S, 2.23.

2.3.9. Synthesis of polymer [P]

To a clear solution of compound **13b** (0.5 g, 0.34 mmol) and compound **9a** (0.319 g, 0.34 mmol) in a mixture of 15 mL of ethanol and 5 mL of chloroform was added sodium ethoxide (0.075 g, 1.39 mmol) solution, in 10 mL of ethanol at room temperature under nitrogen atmosphere. Reaction mixture turned in to orange red color. It was stirred for 12 h. The solvent was distilled off and 10 mL of water was added and stirred for 1 h. The obtained polymer was redissolved in chloroform and poured into 50 mL of methanol. The precipitate was filtered off and dried at 40 °C under vacuum for 24 h to give fluorescent deep orange colored powder.

^{1}H NMR (400 MHz, $CDCl_3$) δ (ppm): 8.1 (d, 2H, Ar–H, J = 8 Hz), 8.0 (d 2H, Ar–H, J = 8 Hz), 6.9–7.6 (m, 6H, aromatic and vinylic), 4.35 (m, 4H, –OCH_2–), 2.0–1.31 (m, 48H, –$(CH_2)_{10}$–), 0.92 (t, 12H, –CH_3, J = 6.8 Hz). IR (KBr, cm^{-1}): 2918, 2850, 1585, 1457, 1055, 949, 723. Element. Anal. Calcd. for C, 69.93; H, 8.80; N, 6.12; S, 7.00. Found: C, 70.15; H, 9.24; N, 6.42; S, 7.25.

3. Results and discussion

3.1. Synthetic plan

Scheme 1 shows the synthetic route for the preparation of new conjugated monomers and their polymerization to the target polymer. The diesters of 3,4-dialkoxy thiophene**s** was readily converted to 3,4-dialkoxythiophene-2,5-carboxydihydrazides **(6a,b)**, by the action of hydrazine hydrate in alcoholic medium. Further, this dihydrazide was tolylated to yield 3,4-bis(dodecyloxy)-*N*′2,*N*′5-bis(4-methylbenzoyl)thiophene-2,5-dicarbohydrazide (**10b)**, which on treatment with phosphorus oxychloride gave corresponding 5,5′-(3,4-bis(dodecyloxy)thiophene-2,5-diyl)bis(2-p-tolyl-1,3,4-oxadiazole) (**11b)** [25] in good yield. This bisoxadiazole compound (**11b**) was then Wohl–Ziegler brominated using *N*-bromosuccinimide (NBS) in carbontertachloride (CCl_4) and the resulting 5,5′-(3,4-bis(dodecyloxy)thiophene-2,5-diyl)bis(2-(4-(bromomethyl)phenyl)-1,3,4-oxadiazole) (**12b**) was further converted to corresponding 5,5′-(3,4-bis(dodecyloxy)thiophene-2,5-diyl)bis(2-(4-triphenylphosphonionmethyl)phenyl)-1,3,4 oxadiazole (**13b**) on treatment with triphenylphosphine in the presence of DMF.

On the other hand co-monomer dialdehyde (**9a**) was prepared by series of reactions as given in Scheme 1. 3-(Thiophen-2-yl)acryloyl chloride was made to react with 3,4-bis (tetradecyloxy)thiophene-2,5-dicarbohydrazide (**6a**) in the presence of pyridine to get 3,4-bis(tetradecyloxy)-*N*′2,*N*′5-bis((Z)-3-(thiophen-2-yl)acryloyl)thiophene-2,5-dicarbohydrazide (**7a**) which was then cyclized using phosphorus oxychloride to yield 5,5′-(3,4-bis(tetradecyloxy)thiophene-2,5-diyl)bis(2-(-2-(thiophen-2-yl)vinyl)-1,3,4-oxadiazole) (**8a)**. In the penultimate step, this compound was converted to the required monomer, viz. (5,5′-(3,4-bis(tetradecyloxy)thiophene-2,5-diyl)bis(1,3,4-oxadiazole-5,2-diyl))bis(ethene-2,1-diyl)dithiophene-2-carbaldehyde (**9a**) by Vilsmeier–Haack reaction using phosphorus oxychloride and DMF. Finally, the target polymer **P** was obtained by Wittig condensation of monomers **9a** and **13b** in the presence of chloroform–ethanol under nitrogen atmosphere [26].

3.2. Characterization

The structures of intermediates were confirmed by elemental analysis and spectroscopic techniques. The structure of 3,4-dialkoxythiophene-2,5-carboxydihydrazides (**6a,b**) were established by its IR and ^{1}H NMR spectra. Its IR spectrum showed sharp peaks at 3412 and 1650 cm^{-1} indicating the presence of –NH_2 and >C=O groups, respectively. ^{1}H NMR spectrum of it displayed peaks at δ 8.3 (s, 2H) and δ 4.9 (s, 4H) for –NH– and –NH_2 protons, respectively. Conversion of bishydrazide **6b** to biscarbohydrazide **10b** was confirmed by the IR spectral and elemental analysis studies. It exhibited sharp peaks at 3245 and 1666 cm^{-1} which indicate the presence of –NH– and >C=O groups, respectively. Further, its ^{1}H NMR spectrum showed peaks at δ 2.38, δ 10.22 and δ 9.71 indicating the presence of the toulal methyl protons and amidic protons, respectively. Formation of compound **10b** from **11b** was established by IR, ^{1}H NMR and mass spectral analyses. The disappearance of bands in the region 3245 and 1666 cm^{-1} and appearance of new band at 1587 cm^{-1} indicate the formation of oxadiazole ring in the molecule. Further, it was confirmed by ^{1}H NMR, it showed disappearance of –NH_2– and –NH– in the spectrum and the aromatic protons were deshielded. Conversion of compound **11b** to **12b** was confirmed by ^{1}H NMR studies and elemental analysis. In its ^{1}H NMR spectrum the disappearance of tolyl methyl protons and appearance of a new peak at δ 4.5 indicates the bromination of methyl groups attached to aromatic rings. Further formation of compound **13b** was confirmed by ^{1}H NMR studies and mass spectral analysis. It showed a peak at δ 5.95 indicates the presence of –CH_2– groups attached to aromatic ring and posphonium group on either side. Formation of compound **7a** was confirmed by IR and ^{1}H NMR spectroscopic technique. It showed intense band at 3310 and 1685 cm^{-1} indicates the presence of –NH– and >C=O groups, respectively. Further ^{1}H NMR spectrum of this compound showed peaks at δ 9.21 and δ 9.98 indicating the formation of amide. Structure of compound **8a** was confirmed by IR, ^{1}H NMR and mass spectral analysis, it showed strong absorption band at 1585 cm^{-1} indicates the formation of oxadiazole ring. ^{1}H NMR spectrum of the compound showed disappearance of amidic protons and it also showed deshielding of aromatic protons due to the formation of oxadiazole ring and it also showed two doublets at δ 7.74 and δ 6.90 corresponding to vinylic protons with coupling constant J = 16 Hz. Mass spectral analysis showed the M+1 peak at 862 which corresponds to the molecular formula $C_{48}H_{68}N_4O_4S_3$. The formation of compound **9a** was confirmed by IR, ^{1}H NMR and elemental analysis. It showed strong absorption band at 1662 cm^{-1} indicates the presence of the aldehydic carbonyl group and it was confirmed by ^{1}H NMR and it showed a peak at δ 9.94 and one of the aromatic protons on the thiophene ring also disappeared from δ 7.29 which confirms the formylation on either side. Elemental analysis showed percentage of elements corresponding to the molecular formula $C_{50}H_{68}N_4O_6S_3$. Finally structure of the polymer was confirmed by elemental analysis, IR and ^{1}H NMR spectroscopic techniques. It showed strong absorption bands at 2918 and 2850 cm^{-1} due to aromatic –C–H stretching and a band at 1585 cm^{-1} which corresponds

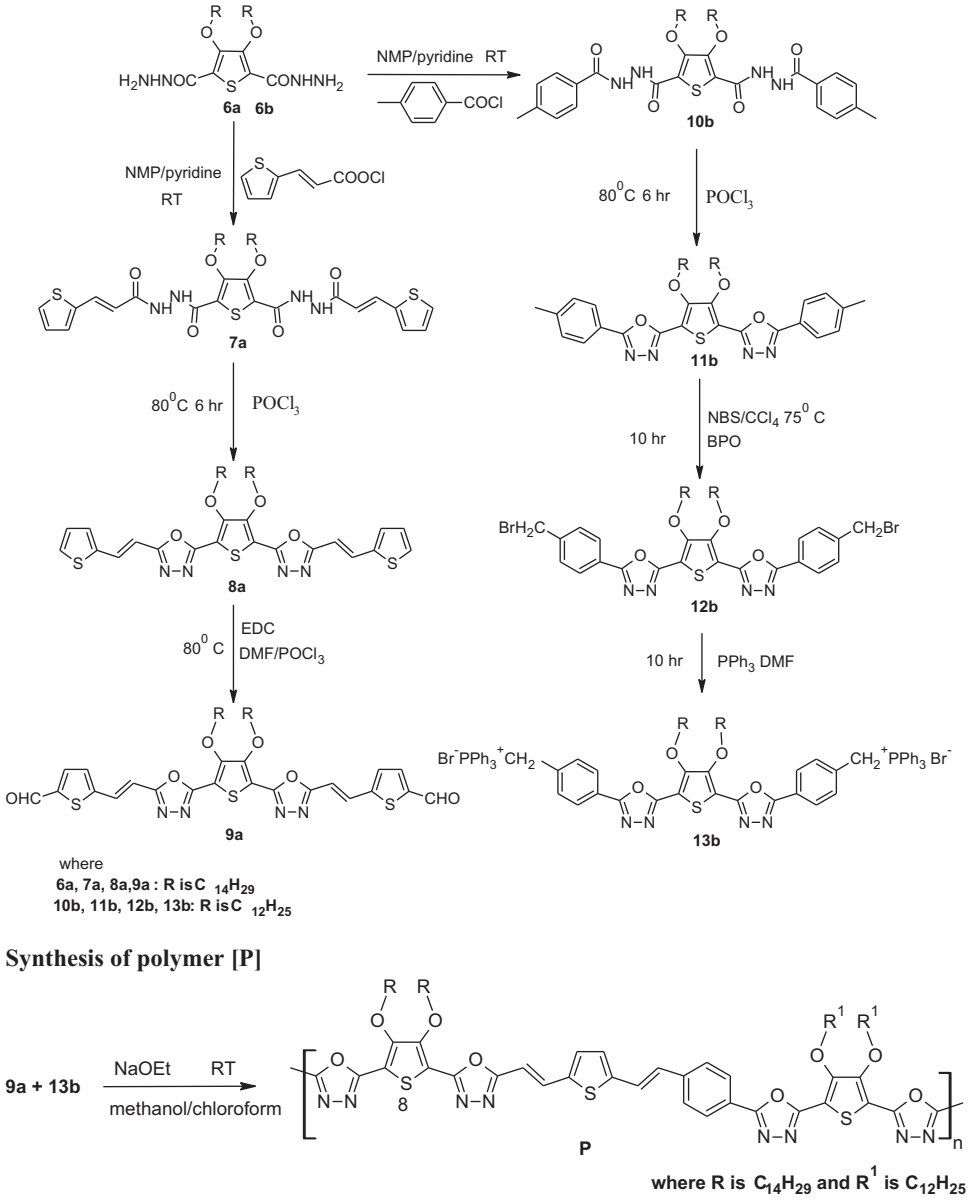

Scheme 1. Synthesis of intermediate, monomers and polymer.

to the oxadiazole –C=N– stretching. In its ^{1}H NMR spectrum, disappearance of peaks due to $-CH_2-PPh_3$ of the monomer clearly indicates the polymerization.

The number average molecular weight of the polymer was found to be 3300 with polydispersity of 2.5. The thermal stability of the polymer was studied by thermogravimetric analysis (TGA) in a nitrogen atmosphere using a 3 °C min^{-1} temperature ramp from 50 to 800 °C. The thermogram showed that the polymer exhibits a high thermal stability losing less than 2–3% weight at 300 °C followed by a drastic degradation process at about 320 °C. The gradual weight loss beyond 300 °C may be attributed to the degradation of the attached alkoxy chains on the thiophene rings. Similar behavior was observed for some of the reported polythiophenes [27]. The newly synthesized polymer is soluble in common organic solvents like chloroform, dichloromethane, tetrahydrofuran and dimethylsufoxide and this polymer showed good processebility and film forming nature. The solubility may be attributed to the presence of bulky alkoxy groups on 3- and 4-positions of thiophene ring (see Fig. 1).

3.3. Electrochemical studies

Cyclic voltammetry (CV) was employed to determine redox potentials of new polymer and then to estimate the HOMO and LUMO levels, which is of importance to determine the band gap. The cyclic voltammogram of the polymer coated on a glassy carbon electrode was obtained by AUTOLAB PGSTAT-30 electrochemical analyzer, using a Pt counter electrode and a Ag/AgCl reference electrode, immersed in the electrolyte [0.1 M (n-Bu)$_4$ NClO4 in acetonitrile] at a scan rate of 25 mV/S [28] (see Fig. 2).

All the measurements were calibrated using ferrocene as standard [29]. As shown in figure, the newly synthesized polymer is electroactive either in the cathodic region or in the anodic region. On sweeping the polymer cathodically, the onset of the n-doping process (reduction) is at the potential of −0.656 V. The cathodic current quickly increases from −0.657 V, and a cathodic peak appears at −1.12 V. This n-doping potential is comparable to other oxadiazole-containing light-emitting polymers [30] and it is even lower than that of 2-(4-biphenylyl)-5-(4-*tert*-butylphenyl)-

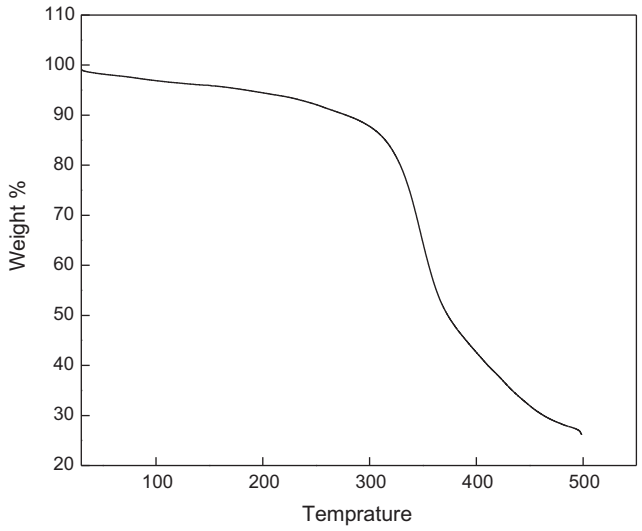

Fig. 1. Thermo gravimetric trace of the polymer **P**.

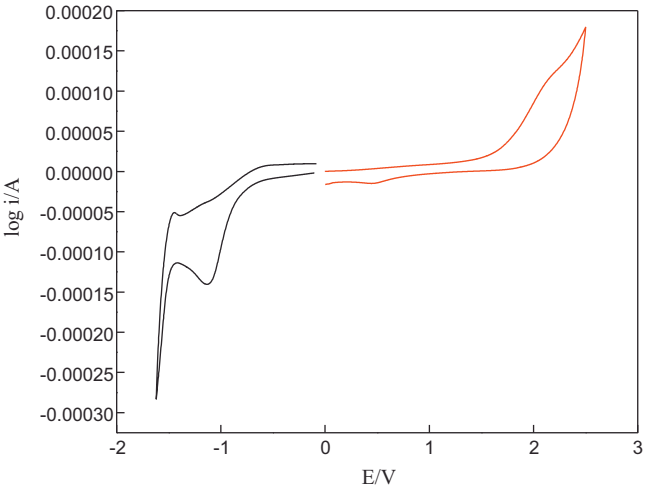

Fig. 2. Oxidation and reduction cyclic voltammetric trace of the polymer **P**.

1,3,4-oxadiazole PBD [31] the most widely used electron-transporting material in PLEDs [32]. Therefore, the new polymer is easier to be reduced than PBD and other oxadiazole-containing light-emitting polymers. For the *p*-doping (oxidation) process, the onset potential for the polymer appeared at 1.518 V and an anodic current peak occurred at 2.14 V. Reversibility of the *p*-doping process is poorer than that of its *n*-doping process. The onset oxidation and reduction potentials were used to estimate the highest occupied molecular orbital (HOMO) and lowest unoccupied molecular orbital (LUMO) energy levels of the polymer **P**. The equations, $E_{HOMO} = -[E_{onset}^{oxd} + 4.4\ \text{eV}]$ and $E_{LUMO} = -[E_{onset}^{red} - 4.4\ \text{eV}]$, where E_{onset}^{oxd} and E_{oxd}^{red} are the onset potentials versus standard calomel electrode (SCE) for the oxidation and reduction of the material referred, were used for the calculation. Electrochemical potentials and energy levels of the polymer are tabulated in Table 1. The HOMO energy level of the polymer was estimated to be −5.918 eV and the LUMO energy level was found to be −3.7 eV. These values are lower than those of cyano-PPV (−3.02) and some aromatic poly (oxadiazole)s (−2.8 to −2.9 eV), indicating that this polymer has very good electron injecting ability [33]. The difference between the *p*-doping and *n*-doping onset potentials was determined to be 2.21 V, this means that the band gap of the polymer obtained from the electrochemical measurement is 2.21 eV. Incorporation of thiophene units into the D–A type conjugated polymer main chain generally decreases the band gap of the polymer by altering the HOMO and LOMO energy levels of the polymer. This is because the introduction of π-excessive thiophene ring increases the effective conjugation length and lowers the band gap of the polymer. These results are comparable with other reported thiophene-oxadiazole containing light-emitting and charge-transporting polymers, which exhibit strong electron-transporting ability. Since the new polymer has good electron-transporting ability comparable to that of PPV, it can be used as emissive material in PLED [34].

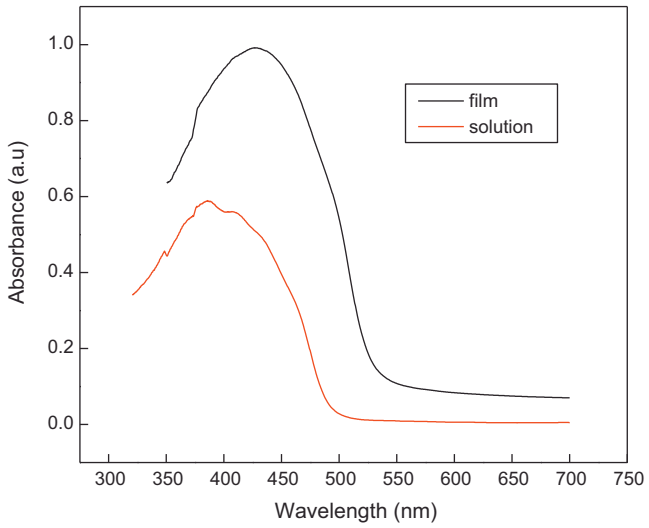

Fig. 3. UV–visible absorption spectra of the polymer **P** in both solution and film state.

3.4. Linear optical properties

Optical property of the polymer was studied by UV–vis and fluorescence spectroscopic studies. The UV–vis absorption and fluorescence emission spectra were recorded both in dilute THF solution and in thin film. The absorption maximum of the polymer in dilute solution is 396 nm, assignable to the π–π* transition resulting from the conjugation between the aromatic rings and nitrogen atoms. The absorption spectrums in thin solid film form showed red shift (431 nm) indicating the presence of inter-chain interactions and inter chain mobility of the excitons and excimers generated within the molecule in solid state (see Fig. 3).

It has been also observed that the polymer showed higher absorption maxima when compared to other reported D–A type conjugated polymers based on oxadiazole-thiophene systems. This is mainly due to introduction of thienylene vinlylene units along the polymer backbone which results in increase in conjugation and reduction in steric hindrance of the bulky alkoxy side chains [34]. The optical band gap (E_g) was calculated from the absorption edge, which was found to be 2.21 eV, which is almost same as the electrochemically determined one. The newly synthesized polymer emits intense orange-red fluorescence at 538 nm in THF solution. The UV–vis and Fluorescence spectra of the polymer in dilute solution

Table 1
Electrochemical potentials, energy levels of the polymer **P**.

Polymer	E_{oxd}	E_{red}	E_{oxd} (onset)	E_{red} (onset)	E_{HOMO} (eV)	E_{LUMO} (eV)	E_g (eV)
P	2.14	−1.12	1.51	−0.65	−5.91	−3.7	2.21

Where E_g is electrochemical bandgap.

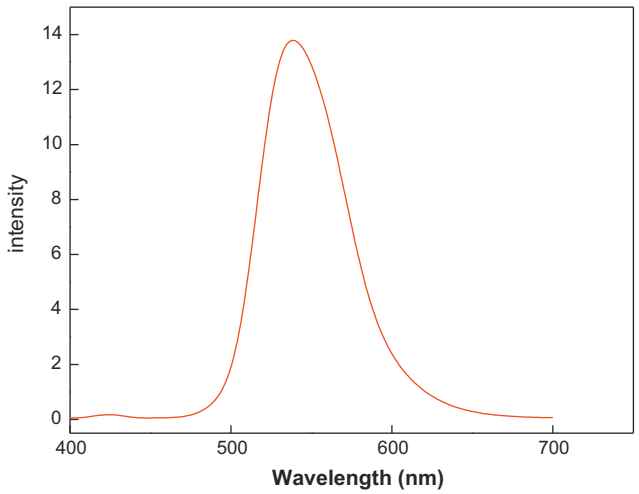

Fig. 4. Fluorescence emission spectrum of the polymer **P** in THF.

are shown in Fig. 4. The fluorescence quantum yield of the polymer in solution was determined using quinine sulfate as standard and it was found to be 35%. These results indicate that the new polymer can be used as fluorescent light emitting material in devices such as light emitting diodes.

3.5. Nonlinear optical properties

3.5.1. Z-scan studies

Fig. 5 shows the open aperture *Z*-scan obtained from sample **P** dissolved in THF. The sample has a linear transmission of about 54% at the excitation wavelength when taken in the 1 mm cuvette. Therefore, strong two-step excited state absorption will happen along with weak genuine two-photon absorption (TPA) in the present case. The net effect is then known as an "effective" TPA process. In addition, the shape of the *Z*-scan curve, where two humps are seen flanking the central valley, is indicative of absorption saturation occurring in the system at input energy densities lower than those where excited state absorption becomes prominent. The nonlinear transmission behavior of the present sample can therefore be

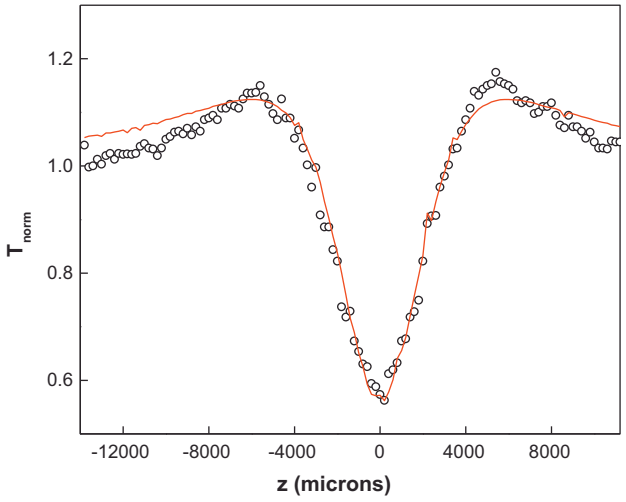

Fig. 5. Open aperture *Z*-scan of sample **P** in THF. Hollow circles are data points while the solid curve is a numerical fit obtained using Eq. (2).

modeled by defining an effective nonlinear absorption coefficient $\alpha(I)$, given by

$$\alpha(I) = \frac{\alpha_0}{1 + (I/I_s)} + \beta I \quad (1)$$

where α_0 is the unsaturated linear absorption coefficient at the wavelength of excitation, and I_s is the saturation intensity (intensity at which the linear absorption drops to half its original value). β is the effective TPA coefficient. For calculating the output laser intensity for a given input intensity, first we numerically evaluate the output intensity from the sample for each input intensity by solving the propagation equation,

$$\frac{dI}{dz'} = -\left[\left(\frac{\alpha_0}{1 + (I/I_s)}\right) + \beta I\right] I \quad (2)$$

using the fourth order Runge–Kutta method. Input intensities for the Gaussian laser beam for each sample position in the *Z*-scan are calculated from the input energy, laser pulse width and irradiation area. Here '*z*' indicates the propagation distance within the sample. The normalized transmittance is then calculated by dividing the output intensity with the input intensity and normalizing it with the linear transmittance. As seen from Fig. 5, there is good agreement between the experimental data and numerical simulation. The numerically estimated values of β and I_s are 3.0×10^{-11} m/W and 6.5×10^{12} W/m^2, respectively. For comparison, under similar excitation conditions, NLO materials like Cu nanocomposite glasses showed effective TPA coefficient values of 10^{-10}–10^{-12} m/W [35], Bismuth nanorods gave 5.3×10^{-11} m/W [36] and CdS quantum dots exhibited 1.9×10^{-9} m/W [37]. These values show that the present sample has an optical nonlinearity comparable to good optical limiters reported in the literature, so that it can find potential applications in optical limiting devices.

In conjugated polymeric system, electrons can move in large molecular orbitals which results from the linear superposition of the carbon p_z atomic orbitals, leading to a very high optical nonlinearity, which increases with the conjugation length [38]. The polymer studied in the present article consists of highly electron rich 3,4-dialkoxy thiophene and strong electron acceptor oxadiazole along with thienyl-vinylene units. Thus, attaching a strong donor to an electron excessive heteroaromatic, such as alkoxy substituted thiophene, and a strong electron acceptor to an electron-deficient heteroaromatic, such as oxadiazole would yield chromophores with significantly enhanced NLO responses because of its D–A architecture [39]. The enhanced third order nonlinearity in the new conjugated polymer is due to the high electron density along the polymer backbone which is easily polarizable as a result of the alternating D–A type of arrangements. The introduction of electron donating alkoxy pendant not only enhanced the donating nature of the thiophene, but also acts as good solubalizng agent for the formed polymer. Further, incorporation of thienyl-vinylene units in between the alkoxy thiophene and oxadiazole systems has decreased the steric strain of bulky alkoxy groups; also it has increased the conjugation path length which in turn enhanced the optical nonlinearity.

3.5.2. DFWM studies

The DFWM signal as a function of pump intensity for sample **P** is shown in Fig. 6. CS_2 is the reference sample for measurement. The signal is proportional to the cubic power of the input intensity as given by the equation,

$$I(\omega)\alpha\left(\frac{\omega}{2\varepsilon_0 cn^2}\right)|\chi^{(3)}|^2 l^2 I_0^3(\omega) \quad (3)$$

where $I(\omega)$ is the DFWM signal intensity, $I_0(\omega)$ is the pump intensity, l is the length of the sample and n is the refractive index of

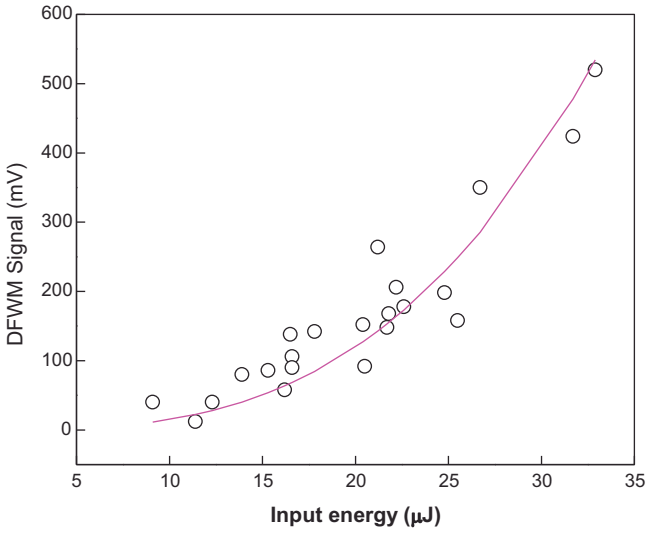

Fig. 6. DFWM signal for the sample. Circles are data points while the solid curve is a cubic fit to the data according to Eq. (3).

the medium. The solid curve in the figure is the cubic fit to the experimental data. $\chi^{(3)}$ can be calculated from the equation

$$\chi^{(3)} = \chi_R^{(3)} \left[\frac{(I/I_0^3)}{(I/I_0^3)_R}\right]^{1/2} \left[\frac{n}{n_R}\right]^2 \frac{l_R}{l} \left(\frac{\alpha l}{(1-e^{-\alpha l})e^{-\alpha l/2}}\right) \quad (4)$$

where the subscript '*R*' refers to the standard reference CS_2. $\chi_R^{(3)}$ is taken to be 4.0×10^{-13} esu [40]. The figure of merit *F*, given by $\chi^{(3)}/\alpha$ is then calculated. *F* is a measure of nonlinear response that can be achieved for a given absorption loss in the medium. The *F* value is useful for comparing the nonlinearity of materials when they are resonantly excited (as in the present case). The $\chi^{(3)}$ value obtained for **P** is 6.25×10^{-12} esu, and the *F* value is 1.21×10^{-12} esu cm, respectively. In comparison, the *F* values are an order of magnitude better than those reported previously in phthalocyanine compounds [40,41] which are materials known to have a high optical nonlinearity.

4. Conclusion

A new D–A type conjugated polymer based on thiophene was synthesized starting from diethyl 3,4-dialkoxythiophene 2,5-dicarboxylates through multistep reactions. The structure of polymer was designed to have thienyl-vinylene as π-conjugated spacer in between a strong electron accepting oxadiazole and an electron donating dialkoxy thiophene moieties. The polymer has well defined structure and good thermal stability. It showed orange color fluorescence under the irradiation of UV light. The optical and electrochemical band gap was found to be 2.21 eV. The third-order optical nonlinearity of the new conjugated polymer **P** was investigated using the nanosecond *Z*-scan and DFWM techniques. A large third-order nonlinearity and optical limiting property were observed in the polymer due to the strong delocalization of π-electrons along the polymer chain. Thus, the presence of a strong conjugating donor, enhanced conjugation path length and planarity of the π-conjugated system are the most important structural factors in governing the electrochemical, spectral as well as nonlinear optical properties of the newly synthesized D–A type polymer. The new polymer possesses a good optical limiting property and high third order susceptibility, and therefore it can be considered as a potential candidate for optoelectronics applications.

Acknowledgements

The authors are grateful to RRI, Bangalore, NMR Research Centre, CDRI, Lucknow, IISc, Bangalore, STIC Cochin and SAIF Gujarat for providing instrumental analyses.

References

[1] K.R. Yoon, N.M. Byun, H. Lee, Synth. Met. 157 (2007) 603.
[2] J. Hao, M.J. Han, K. Guo, Y. Zhao, L. Qiu, Y. Shen, X. Meng, Mater. Lett. 62 (2008) 973.
[3] A. Carella, A. Castaldo, R. Centore, A. Fort, A. Sirigu, J. Chem. Perkin Trans. 2 (2002) 1791.
[4] V.P. Rao, A.K.–Y. Jen, K.Y. Wong, K.J. Drost, Tetrahedron Lett. 34 (11) (1993) 1747.
[5] R.M.F. Batista, S.P.G. Costa, M. Belsley, M.M. Raposo, Tetrahedron 63 (2007) 9842.
[6] V.P. Rao, A.K.–Y. Jen, K.Y. Wong, K.J. Drost, Tetrahedron Lett. 34 (1993) 1747.
[7] A. Abbotto, S. Bradamante, A. Facchetti, G.A. Pagani, J. Org. Chem. 62 (17) (1997) 5755.
[8] S. Yuquan, Z. Yuxia, L. Zao, W. Jianghong, Q. Ling, L. Shixiong, Z. Jianfeng, Z. Jiayun, J. Chem. Soc., Perkin Trans. 1 (1999) 3691.
[9] C.W. Dirk, H.E. Katz, M.L. Schilling, L.A. King, Chem. Mater. 2 (1990) 700.
[10] S.M. Tambe, A.A. Kittur, S.R. Inamdar, G.R. Mitchell, M.Y. Kariduraganavar, Opt. Mater. 31 (2009) 825.
[11] W.N. Leng, Y.M. Zhou, Q.H. Xu, J.Z. Liu, J. Polym. 42 (2001) 9253.
[12] R. Centore, A. Tuzi, B. Panunzi, Z. Kristallogr. 212 (1997) 890.
[13] P. Ambrosanio, R. Centore, S. Concilio, B. Panunzi, A. Sirigu, N. Tirelli, J. Polym. 40 (1999) 4923.
[14] T. Cassano, R. Tommasi, F. Babudri, Opt. Lett. 27 (2002) 2176.
[15] P.R. Varanasi, A.K.Y. Jen, J. Chandrasekhar, I.N.N. Namboothiri, A. Rathna, J. Am. Chem. Soc. 118 (1996) 12443.
[16] F. Effenberger, F. Wuerthner, F. Steybe, J. Org. Chem. 60 (1995) 2082.
[17] D. Udayakumar, A.V. Adhikari, Synth. Met. 156 (2006) 1168.
[18] D. Udayakumar, A.V. Adhikari, Opt. Mater. 29 (2007) 1710.
[19] A.J. Epstein, J.W. Blatchford, Z.H. Wang, S.W. Jessen, D.D. Gebler, L.B. Lin, Synth. Met. 78 (1996) 253.
[20] M. Sheik-Bahae, A.A. Said, T. Wei, IEEE J. Quantum Electron. 26 (1990) 760.
[21] J.M. Hales, J.W. Perry, in: S.-S. Sun, L.R. Dalton (Eds.), Introduction to Organic Electronic and Optoelectronic Materials and Devices, CRC Press, Boca Raton, FL, 2008.
[22] M. Hochberg, T. Baehr-Jones, G.X. Wang, M. Shearn, K. Harvard, J.D. Luo, B.Q. Chen, Z.W. Shi, R. Lawson, P. Sullivan, A.K.Y. Jen, L. Dalton, A. Scherer, Nat. Mater. 5 (2006) 703–709.
[23] S.H. Chi, J.M. Hales, C. Fuentes-Hernandez, S.Y. Tseng, J.Y. Cho, S.A. Odom, Q. Zhang, S. Barlow, R.R. Schrock, S.R. Marder, B. Kippelen, J.W. Perry, Adv. Mater. 20 (2008) 3199–3203.
[24] M. Sheik-Bahae, M.P. Hasselbeck, OSA Handbook of Optics, Optical Society of America, 2000.
[25] T.-Y. Wu, N.-C. Lee, Y. Chen, Synth. Met. 139 (2003) 263.
[26] C.S. Wang, M. Kilitziraki, J.A.H. Macbride, M.R. Bryce, L.E. Horburgh, A.K. Sheridan, Adv. Mater. 12 (2000) 217.
[27] G. Gustafsson, Ignanas, W.R. Salaneck, J. Laakso, M. Loponen, T. Taka, J.-E. Sterholm, H. Stubb, T. Hjertberg, in: J.L. Breĭdas, R. Silbey (Eds.), Conjugated Polymers, Kluwer Academic, Dordrecht, The Netherlands, 1991, p. 315.
[28] Q. Sun, H. Wang, Y. Yang, Li, J. Mater. Chem. 13 (2003) 800.
[29] J. Pommerehe, H. Vestweber, W. Guss, R.F. Mahrt, H. Bassler, M. Porsch, J. Daub, Adv. Mater. 7 (1995) 55.
[30] M. Strukelji, F. Papadimitrakooulous, T.M. Miller, L.J. Rothberg, Science 267 (1995) 1969.
[31] S. Janietz, A. Wedel, Adv. Mater. 9 (1997) 403.
[32] L.J. Rothberg, A.J. Lovinger, J. Mater. Res. 11 (1996) 3174.
[33] D.W. DeLeeuw, M.M.J. Simenon, A.B. Brown, R.E.F. Einerhand, Synth. Met. 87 (1997) 53.
[34] B. Zhao, D. Liu, L. Peng, H. Li, P. Shen, N. Xiang, Y. Liu, S. Tan, Eur. Polym. J. 45 (2009) 2079–2086.
[35] B. Karthikeyan, M. Anija, C.S. Suchand sandeep, T.M. Muhammad Nadeer, R. Philip, Opt. Commun. 281 (2008) 2933.
[36] S. Sivaramakrishnan, V.S. Muthukumar, S. Sivasankara Sai, K. Venkataramanaiah, J. Reppert, A.M. Rao, M. Anija, R. Philip, N. Kuthirummal, Appl. Phys. Lett. 91 (2007) 093104.
[37] P.A. Kurian, C. Vijayan, K. Sathiyamoorthy, C.S. SuchandSandeep, R. Philip, Nano Res. Lett. 2 (2007) 561.
[38] T. Cassano, R. Tommasi, M. Tassara, F. Babudri, A. Cardone, G.M. Farinola, F. Naso, Chem. Phys. 272 (2001) 111.
[39] T.L. Gilchrist, Heterocyclic Chemistry, Wiley, New York, 1985.
[40] J.S. Shirk, J.R. Lindle, F.J. Bartoli, M.E. Boyle, J. Phys. Chem. 96 (1992) 5847.
[41] R. Philip, M. Ravikanth, G. Ravindra Kumar, Opt. Commun. 165 (1999) 9.